

# PHASE EQUILIBRIUM MODELING IN THE HYDROGENATION OF VEGETABLE OILS AND DERIVATIVES

Selva Pereda\*, Laura Rovetto, Susana B. Bottini and Esteban A. Brignole

PLAPIQUI- Univesidad Nacional del Sur, CONICET  
Camino La Carrindanga, Km 7, C.C. 717, 8000 Bahía Blanca, Argentina  
Tel: +54 291 481700 Ext: 234 – FAX: +54 291 481700 e-mail: spered@plapiqui.edu.ar

Submitted to: JAOCS - July 14, 2005

Topical Area: Analytical and Physical Chemistry

**Keywords:** *vegetable oil hydrogenation, fatty ester hydrogenolysis, thermodynamic modeling, GCA-EoS*

## PHASE EQUILIBRIUM MODELING IN THE HYDROGENATION OF VEGETABLE OILS AND DERIVATIVES

S. Pereda\*, L. Rovetto, S.B. Bottini and E.A. Brignole

PLAPIQUI- Universidad Nacional del Sur, CONICET

Camino La Carrindanga, Km 7, C.C. 717, 8000 Bahía Blanca, Argentina

**Abstract:** The main tool required to carry out phase equilibrium engineering of a given process is an adequate thermodynamic model tuned to the range of process operating conditions of the working system. In the present work the Group Contribution with Association Equation of State (GCA-EoS) is used to model the phase behavior of reacting mixtures typical of the hydrogenation of vegetable oils and derivatives at supercritical or high-pressure conditions. Previous work showed that the GCA-EoS is able to model vapor–liquid, liquid–liquid and vapor-liquid-liquid equilibria with a single set of parameters.

**Keywords:** vegetable oil hydrogenation, fatty ester hydrogenolysis, thermodynamic modeling, GCA-EoS

Hydrogenation is a major chemical industrial process. A wide variety of chemicals are obtained by heterogeneous catalytic hydrogenation. Two important gas-liquid catalytic hydrogenation processes in the oil industry are the manufacture of margarine and shortenings from vegetable oils and the production of fatty alcohols from alkyl esters, such as methyl esters:



It has been proved that these reactions can be carried out under homogeneous fluid conditions by the addition of an appropriate supercritical solvent such as propane, leading to improved processes with higher reaction rates and selectivities (1, 2, 3). A suitable thermodynamic model, capable of predicting the phase boundaries and fluid phase behavior of the working mixtures, is the critical tool for process design and optimization.

Group contribution methods are an efficient way to model the phase equilibrium properties of mixtures including gases, triglycerides and derivatives, because a large number of systems can be represented by a limited number of functional groups. For example, besides

hydrogen, the mixtures relevant to the hydrogenation of vegetable oils and fatty esters contain only five different functional groups: alkyl ( $\text{CH}_3$  and  $\text{CH}_2$ ), olefin ( $\text{CH}=\text{CH}$ ), triglyceride ( $\text{TG} = (\text{CH}_2\text{COO})_2\text{CHCOO}$ ), ester ( $\text{CH}_2\text{COO}$ ) and alcohol ( $\text{CH}_2\text{OH}$ ). The Group Contribution Equation of State (4), extended to fatty oils (5) and associating compounds (6, 7, 8), is applied in the present work to model these reaction mixtures. A brief description of the model is given in the Appendix. Recent experimental data obtained by Rovetto et al. for propane + hydrogen + tripalmitin (9) and propane + hydrogen + alcohols/fatty esters (10, 11) are used to tune the model parameters and to test its predictive capacity. The modeling results are essential for the phase equilibrium engineering of reactors for the supercritical or high-pressure hydrogenation of oils and derivatives.

Table 1 shows the parameters involved in each term of the Group Contribution with Association Equation of State (GCA-EoS). The table also reports which parameters should be estimated in each case. The hard sphere critical diameter ( $d_c$ ) is a parameter related to molecular size. In general this parameter is obtained from critical properties and vapor pressure data of pure compounds. However, this type of information is not available for low-volatile molecules like triglycerides. Bottini et al (5) presented a correlation for the computation of  $d_c$ , obtained from values of infinite dilution activity coefficient of alkanes in high molecular weight paraffins and triglycerides. Table 2 shows the  $d_c$  values and the critical temperatures of the different components studied in this work.

## **RESULTS AND DISCUSSION**

### ***Phase equilibrium modeling in the hydrogenation of vegetable oils***

Skjold-Jorgensen (1) originally determined the interaction parameters between hydrogen and the paraffin group on the basis of experimental data on hydrogen solubility in alkanes containing up to 16 carbon atoms. These parameters had to be revised in order to get

a good correlation of hydrogen solubility in molecules with more than 40 carbon atoms. The large number of paraffin groups in the triglyceride molecule originates big differences in the predictions with small changes in the  $H_2$ - $CH_2$  interaction parameter.

New binary interaction parameters hydrogen -paraffin and hydrogen - triglyceride were estimated on the basis of the new experimental data from Rovetto et al (9). Table 3 reports the new set of binary interaction parameters obtained by fitting  $N= 63$  data points with a standard deviation  $SDV = 1.263\%$  in the calculated hydrogen liquid molar fractions. The GCA-EoS correlation of hydrogen solubility in tripalmitin is very good, as shown in Figure 1.

For reactions carried out under supercritical propane, the behavior of mixtures containing this solvent must be studied. The phase equilibrium of triglyceride + propane binary mixtures is of type IV in the classification of van Konynenburg and Scott (12). In this type of phase behavior a region of liquid immiscibility is observed in the near critical region of propane ( $T_c=369.8$  K). For example, Coorens et al (13) report values of 349 K and 370 K for the lower and upper critical end points, respectively, of the system propane + tripalmitin. Espinosa et al (14) fitted the model parameters in order to correctly describe the phase equilibria of mixtures of propane with triglycerides.

Figure 2 shows GCA-EoS phase boundaries predictions for the system hydrogen+propane+tripalmitin at 360 K and 4 MPa. Under these conditions the model predicts phase immiscibility in the three binaries. The concentration of triglyceride in the  $l_2$  liquid phase is negligible; therefore, the saturation line  $l_2$  is almost coincident with the hydrogen+propane binary axis. At higher hydrogen concentrations a vapor phase is found and a three-phase equilibrium region  $l_1l_2g$  is obtained. For the same reason stated before, the line  $l_2g$ , lies virtually over the axis  $H_2$ -propane. A region of complete miscibility for this ternary system can be obtained by increasing the temperature above the critical temperature of

propane and selecting a pressure above 100 bar. By this way a region suitable for single-phase hydrogenation can be reached (2).

Predictions for the ternary  $H_2$ +propane+tripalmitin are compared with experimental data in Figure 3 and 4. The agreement with the experimental data is quite good. Figure 3 shows how the slope of the pressure vs. temperature phase diagrams changes with the concentration of propane. At low propane concentrations the saturation pressure decreases with temperature, following the typical behavior of mixtures of hydrogen + liquid substrates. At higher propane concentrations the saturation pressure increases with temperature, in agreement with the expected behavior of mixtures of propane with liquid substrates.

The correlations and predictions shown in this section were performed using the parameters reported in Table 3 for the interactions  $H_2/CH_2$  and  $H_2/TG$  and those given by Skjold-Jorgensen (1) for  $H_2/C_3H_8$  and by Espinosa et al. (14) for  $CH_2/TG$ . This last paper also reports the binary interaction parameters between  $CH=CH$  and  $TG$ , which are required to predict the phase behavior of mixtures containing unsaturated triglycerides.

### ***Phase equilibrium modeling of the hydrogenolysis of fatty acid methyl esters.***

Following a similar procedure, the GCA-EoS model was extended to cover the phase equilibrium engineering needs for the hydrogenolysis of methyl palmitate to hexadecanol. In this case the number of components present in the mixture is greater and there is a significant change in the chemical nature of the mixture as the reaction proceeds from the fatty ester to the fatty alcohol + methanol products. The critical diameter and critical temperature of pure components are reported in Table 2. The required binary interaction parameters were obtained by fitting experimental data on binary mixtures of hydrogen, propane and butane with either methyl palmitate or hexadecanol (9, 11, 15). Low-pressure data for mixtures between esters and alcohols (16, 17) were also used. Again, the amount of experimental

information is very limited making it difficult to verify the predicting capability of the model. For this reason, only a fraction of the binary vapor-liquid equilibrium isopleths was applied in the estimation of parameters. The rest of the binary and ternary experimental data was used to validate the GCA-EoS phase equilibrium predictions. The dashed lines in Figures 5 to 11 represent data correlation and the solid lines are predictions.

Table 4 reports the binary interaction parameters estimated in the present work. The remaining parameters required for phase equilibrium correlation and prediction in these systems were obtained from Skjold-Jorgensen (1) for the interactions H<sub>2</sub>-alkyl groups and from Gros et al. (18) for the interactions CH<sub>2</sub>OH-alkyl groups.

*Binary systems: hydrogen with methyl palmitate and n-hexadecanol*

Figure 7 shows the bubble pressures of the systems H<sub>2</sub>+methyl palmitate and H<sub>2</sub>+hexadecanol. Comparing the bubble pressures of each system for isopleths with similar hydrogen compositions, it is possible to observe that the bubble pressures of hexadecanol are higher than those of methyl palmitate. This indicates that hydrogen is less soluble in the fatty alcohol. This phenomenon was also observed by van den Hark et al. (1), who found problems of phase split in the course of the hydrogenolysis process, due to the decrease of hydrogen solubility as the reaction proceeds to the formation of fatty alcohol.

*Binary systems: propane and butane with methyl palmitate and n-hexadecanol*

Figure 5 shows the correlation and prediction of phase equilibria for the binary systems propane+methyl palmitate and propane+hexadecanol, together with experimental data (10, 11). In general, a very good agreement is obtained. However, greater deviations are found in the prediction of dew points. This is due to the great sensitivity of dew-points to the fugacity computation of heavy compounds. It has been observed that equations of state in

general have difficulties in predicting the solubility of heavy compounds in a high-pressure vapor phase.

Figure 6 shows the correlation and predictions of binary phase equilibria for butane+methyl palmitate and butane+hexadecanol. The agreement with experimental data (15) for both systems is very good.

#### Binary systems: alcohol with esters

The interaction parameters between the ester ( $\text{CH}_2\text{COO}$ ) and alcohol ( $\text{CH}_2\text{OH}$ ) groups were determined by fitting the low-pressure isothermal data reported by Fernández et al (16, 17). Table 5 gives the number of data points and the temperature range of each system, together with the average errors in pressure and vapor phase compositions. These deviations between predicted and experimental data were obtained from bubble pressure calculations at a given temperature and liquid composition.

The predictive capability of the model was verified by comparison with isobaric data measured by Susial and Ortega (19, 20) and by Ortega et al. (21) for the system ethanol+methylbutanoate and butanol+methylpropanoate (see Figure 8 ).

#### Predictions for ternary systems

Rovetto et al. (10, 11) reported equilibrium data for ternary systems of interest in the hydrogenolysis of methyl palmitate. The effect of propane concentration on the phase behavior of the system hydrogen + propane + methyl palmitate was determined at a constant ester/hydrogen molar ratio of 8.7, for propane molar fractions in the range 0 - 77%. Figure 9 shows the experimental and predicted bubble pressures of this system. At low propane concentration the isopleths have a negative slope, typical of hydrogen solubility behavior (i.e., solubility increases with temperature). At higher propane concentrations the system

presents the standard behavior of a pressure increase with temperature. It is interesting to note that there is a propane concentration range where the system pressure is almost independent of temperature. The model predicts very closely this behavior and the composition at which the change in slope takes place.

The results reported by van den Hark (1) and the phase equilibrium engineering carried out by Pereda et al. (2) for this system, indicate that high propane concentrations are required to perform the reaction in a homogeneous fluid medium. The predictions for ternary mixtures of propane+methyl palmitate+n-hexadecanol and propane+hexadecanol+methanol at high propane concentrations are shown in Figure 10a and Figure 10b respectively.

Finally, the phase equilibrium predictions for the ternaries hydrogen+methyl palmitate+ propane and for hydrogen+n-hexadecanol+propane are represented in Figure 11a and b respectively. In both cases the molar ratio hydrogen/substrate was kept constant at a value equal to four. All isopleths depict a minimum in pressure, close to the mixture critical point. The model almost quantitatively predicts this unusual behavior. The system hydrogen+n-hexadecanol+propane also exhibits a region of liquid–liquid–vapor equilibrium that is also qualitatively predicted by the model. Peters (22) has shown that binary mixtures of n-alkanols with propane exhibit partial liquid miscibility starting with carbon number 18. However, the addition of hydrogen to the system has an antisolvent effect and the liquid–liquid–vapor behavior is observed for n-hexadecanol. Again the model gives a correct qualitative description of the three-phase region. It is interesting to note that the narrow range of liquid-liquid-vapor behavior was experimentally found by studying the three phase conditions predicted by the thermodynamic model.



## CONCLUSIONS

A flexible group contribution model has been tuned to predict phase equilibria in high-pressure hydrogenation processes of fatty oils and derivatives. New interaction parameters have been estimated. The experimental data are well correlated and accurate predictions are obtained. The complex phase behavior of these systems can be represented with a single set of model parameters. Minima in pressure and regions of liquid–liquid and liquid–liquid–vapor equilibria are predicted in agreement with experimental data.

## REFERENCES

1. van den Hark, S., The use of supercritical fluids to reduce the number of phases in catalytic hydrogenation: the reaction of fatty acid methyl esters to fatty alcohols, PhD Thesis - Chalmers University of Technology - Sweden (2000).
2. Pereda, S., S.B. Bottini, and E.A. Brignole, Phase equilibrium engineering of supercritical hydrogenation reactors, *AIChE J.*, 48: 2635-2645 (2002).
3. Pereda, S., S.B. Bottini, and E.A. Brignole, Supercritical fluids and phase behavior in heterogeneous gas–liquid catalytic reactions, *Applied Catalysis A: General*, 281: 129-137 (2005).
4. Skjold-Jørgensen, S., Group contribution equation of state (GC-EOS): A predictive method for phase equilibrium computations over wide ranges of temperature and pressures up to 30 Mpa, *Ind. Eng. Chem. Res.*, 27: 110-118 (1988).
5. Bottini, S.B., T. Fornari and E.A. Brignole, Phase equilibrium modeling of triglycerides with near critical solvents, *Fluid Phase Equilibria*, 158-160: 211-218 (1999).
6. Zabaloy, M.S., G.D.B. Mabe, S.B. Bottini, and E.A. Brignole, Vapor – liquid equilibria in ternary mixtures of water – alcohol – non-polar mixtures, *Fluid Phase Equilibria*, 83: 159-166 (1993).
7. Gros, H.P, S.B. Bottini and E.A. Brignole, A group contribution equation of state for associating mixtures, *Fluid Phase Equilibria*, 116: 537-544 (1996).
8. Ferreira, O., E.A. Macedo, E.A. Brignole, Modelling of phase equilibria for associating mixtures using an equation of state, *J. Chem. Thermodynamics*, 36: 1105–1117 (2004).
9. Rovetto, L.J., S.B. Bottini, E.A. Brignole, and C.J. Peters, Supercritical hydrogenation processes. Experimental results on the fluid phase behavior of binary and ternary mixture of hydrogen, propane and tripalmitin, *J. Supercritical Fluids*, 25: 165-176 (2003).
10. Rovetto, L.J., S.B. Bottini, and C.J. Peters, Phase equilibrium data on binary and ternary mixtures of methyl palmitate, hydrogen and propane, *J. Supercritical Fluids*, 31: 111-121 (2004).

11. Rovetto, L.J., S.B. Bottini, E.A. Brignole, and C.J. Peters, Supercritical hydrogenolysis of fatty acid methyl esters: phase equilibrium measurements on selected binary and ternary systems, *J. Supercritical Fluids*, in press: - (2005).
12. van Konynenburg, P.H., and R.L. Scott, Critical lines and phase equilibria in binary van der Waals mixtures, *Phil. Trans.*, 298: 495-540 (1980).
13. Coorens, H.G.A., C.J. Peters, and J. De Swaan Arons, Phase equilibria in binary mixtures of propane and tripalmitin, *Fluid Phase Equilibria*, 40: 135-151 (1988).
14. Espinosa, S., T. Fornari, S.B. Bottini, and E.A. Brignole, Phase equilibria in mixtures of fatty oils and derivatives with near critical fluids using the GCA-EOS model, *Journal of Supercritical Fluids*, 23, 91-102 (2002).
15. Brands, D.S., The hydrogenolysis of esters to alcohols over copper containing catalysts, Ph.D. Thesis - Universiteit van Amsterdam, Amsterdam - The Netherland (1998).
16. Fernandez, J., C. Berro, and M.I. Paz Andrade, Excess thermodynamics functions of 1-propanol+methyl propanoate and 1-propanol+methyl butanoate systems, *Fluid Phase Equilibria*, 20: 145-153 (1985).
17. Fernandez, J. C. Berro, and A. Pénélox, Excess gibbs energies and excess volumens of some alcohol-methyl ester binary mixtures, *J. Chem. Eng. Data*, 32: 17-22 (1987).
18. Gros, H.P, S.B. Bottini, and E.A. Brignole, High pressure phase equilibrium modeling of mixtures containing associating compounds and gases, *Fluid Phase Equilibria*, 139: 75-87 (1997).
19. Susial, P., and J. Ortega, Vapor-liquid equilibrium measurements for methyl propanoate-ethanol and methyl propanoate-propan-1-ol at 101.32 kPa, *J. Chem. Eng. Data*, 34: 247-250 (1989).
20. Susial, P., and J. Ortega, Isobaric vapor-liquid equilibria in the system methyl propanoate+n-butyl alcohol, *J. Chem. Eng. Data*, 38: 647-649 (1993).
21. Ortega, J., P. Susial, and C. Alfonso, Isobaric vapor-liquid equilibrium of methyl butanoate with ethanol and 1-propanol binary systems, *J. Chem. Eng. Data*, 35: 216-219 (1990).
22. Peters, C.J., *Supercritical fluids. Fundamentals for application. Multiphase equilibria in near-critical solvents*, Kluwer Academic Publisher. Editors: Kiran E. and Levelt Sengers M.H. (1994).

## APPENDIX

The GCA-EOS model is based on a group contribution expression of the configurational Helmholtz function,  $A^C$ . All thermodynamic phase equilibrium properties may be derived from  $A^C$  by differentiation with respect to composition or volume.

The total Helmholtz energy has two parts. The first term  $A^{ideal}$  describes the ideal gas behavior and the second part, the configurational  $A^C$  Helmholtz function, takes into account the intermolecular forces through a repulsive or free volume term  $A^{fv}$ , an attractive term  $A^{att}$  and an associative contribution  $A^{assoc}$ :

$$A = A^{ideal} + (A^{fv} + A^{att} + A^{assoc})$$

The free volume term is modeled by assuming a hard spheres behavior of the molecules, characterized by the hard sphere diameter  $d_i$ . A Carnahan-Starling type of hard sphere expression for mixtures is adopted:

$$(A/RT)^{fv} = 3(\lambda_1\lambda_2/\lambda_3)(Y-1) + (\lambda_2^3/\lambda_3^2)(-Y+Y^2 - \ln Y) + n \ln Y$$

with:

$$Y = \left(1 - \frac{\pi\lambda_3}{6V}\right)^{-1} \quad \text{y} \quad \lambda_k = \sum_i^{NC} n_i d_i^k$$

where  $n_i$  is the number of moles of component  $i$ ,  $NC$  is the number of components and  $V$  is the total volume.

The following generalized correlation is used for the temperature dependence of the hard sphere diameter:

$$d_i = 1.065655 d_{ci} \{1 - 0.12 \exp[-2T_{ci}/(3T)]\}$$

where  $d_c$  is the value of the hard-sphere diameter at the critical temperature  $T_c$  of pure component  $i$ .

The attractive contribution to the Helmholtz energy is evaluated with a group contribution, density-dependent NRTL expression:

$$(A / RT)^{att} = - \frac{z}{2} \sum_i^{NC} n_i \sum_j^{NG} v_j^i q_j \sum_k^{NG} (\theta_k g_{kj} \tilde{q} \rho) / \sum_l^{NG} \theta_l \tau_{lj}$$

where:

$$\theta_j = (q_j / q) \sum_i^{NC} n_i v_j^i \quad q = \sum_i^{NC} n_i \sum_j^{NG} v_j^i q_j$$

$$\tau_{ij} = \exp[\alpha_{ij} \Delta g_{ij} \tilde{q} / (RTV)]$$

$$\Delta g_{ij} = g_{ij} - g_{jj}$$

$v_j^i$  is the number of groups of type  $j$  in molecule  $i$ ,  $q_j$  the number of surface segments assigned to group  $j$ ,  $\theta_k$  the surface fraction of group  $k$ ,  $\tilde{q}$  the total number of surface segments,  $z$  the number of nearest neighbors to any segment (set equal to 10),  $g_{ij}$  the attraction energy parameter for interactions between groups  $i$  and  $j$ , and  $\alpha_{ij}$  the non-randomness parameter.

The interactions between unlike groups are calculated from:

$$g_{ij} = k_{ij} (g_{ii} g_{jj})^{1/2} \quad (k_{ij} = k_{ji})$$

with the following temperature dependences for the energy and interaction parameters:

$$g_{jj} = g_{jj}^* \left( 1 + g'_{jj} (T/T_j^* - 1) + g''_{jj} \ln(T/T_j^*) \right)$$

and

$$k_{ij} = k_{ij}^* \{ 1 + k'_{ij} \ln[2T / (T_i^* + T_j^*)] \}$$

where  $g_{jj}^*$  is the interaction parameter at the reference temperature  $T_i^*$ .

The Helmholtz function due to association is calculated with a modified form of the expression used in the SAFT equation, and is formulated in terms of associating groups:

$$\frac{A^{assoc}}{RT} = \sum_{i=1}^{NGA} n_i \left[ \sum_{k=1}^{M_i} \left( \ln X^{(k,i)} - \frac{X^{(k,i)}}{2} \right) + \frac{1}{2} M_i \right]$$

where  $NGA$  represents the number of associating groups,  $n_i$  the total number of moles of associating group  $i$ ,  $X^{(k,i)}$  the mole fraction of group  $i$  not bonded at site  $k$  and  $M_i$  the number of associating sites assigned to group  $i$ . The number of moles of the associating group is:

$$n_i = \sum_{m=1}^{NC} \nu_{assoc}^{(i,m)} n_m$$

where  $\nu_{assoc}^{(i,m)}$  represents the number of times associating group  $i$  is present in molecule  $m$  and  $n_m$  the total number of moles of molecules  $m$ ; the summation includes all the  $NC$  components in the mixture.

The mole fraction of group  $i$  not bonded at site  $k$  is determined from:

$$X^{(k,i)} = \left[ 1 + \sum_{j=1}^{NGA} \sum_{l=1}^{M_j} \rho_j X^{(l,j)} \Delta^{(k,i,l,j)} \right]^{-1}$$

$X^{(k,i)}$  depends on the molar density of the associating group  $j$   $\rho_j = n_j / V$  and on the association strength between site  $k$  of group  $i$  and site  $l$  of group  $j$ :

$$\Delta^{(k,i,l,j)} = \frac{n_j}{V} \kappa^{(k,i,l,j)} \left[ \exp(\epsilon^{(k,i,l,j)} / KT) - 1 \right]$$

The associating strength is function of the characteristic association parameters  $\zeta$  (association energy, K) and  $\kappa$ . (associating volume, cm<sup>3</sup>/mol)

## LIST OF TABLES

**Table 1.** GCA-EoS model parameters.

**Table 2:** Pure component properties.

**Table 3:**GCA-EoS binary interactions parameters.

**Table 4:** GCA-EoS binary interaction parameters

**Table 5:** Systems used for parameter estimation between the CH<sub>2</sub>COO and CH<sub>2</sub>OH groups.

## LIST OF FIGURES

**Figure 1:** Phase diagram of the binary system hydrogen+tripalmitin. Dots: experimental data (9). — GCA-EoS correlation.

**Figure 2:** Immiscibility region for the ternary system hydrogen+tripalmitin (PPP)+propane at 360 K and 4 MPa.

**Figure 3:** Phase diagram of the ternary system hydrogen+propane+tripalmitin(PPP) at a constant molar ratio  $x(\text{PPP})/x(\text{H}_2) = 4.15$  — GCA-EoS predictions. Dots: experimental data (9).

**Figure 4:** Phase diagram of the ternary system hydrogen+propane+tripalmitin at a constant molar ratio  $x(\text{C}_3\text{H}_8) / x(\text{PPP}) = 7$ . Dots: experimental data (9). — GCA-EoS predictions.

**Figure 5:**(a) Phase diagram of the binary system methyl palmitate+propane.  
(b) Phase diagram of the binary system hexadecanol+propane. Dots: experimental data (10, 11). - - - GCA-EoS correlation. — GCA-EoS predictions.

**Figure 6:**(a) Phase diagram of the binary system methyl palmitate(MP)+butane.  
(b) Phase diagram of the binary system hexadecanol(HD)+butane. Dots: experimental data (15). - - - GCA-EoS correlation. — GCA-EoS predictions.

**Figure 7:**(a) Bubble points of the binary system methyl palmitate + hydrogen  
(b) Bubble points of the binary system hexadecanol + hydrogen. Dots: experimental data (10, 11). - - - GCA-EoS correlations. — GCA-EoS predictions.

**Figure 8:**(a) Vapor-liquid equilibria of the binary system ethanol+methylbutanoate.  
(b) Vapor-liquid equilibria of the binary system butanol+methylpropanoate. Dots: experimental data (20, 21). — GCA-EoS predictions.

**Figure 9:**Bubble pressure of the ternary system methyl palmitate+hydrogen+propane ( $x_{\text{MP}}:x_{\text{H}_2} = 8.7$ ). Dots: experimental data (10). — GCA-EoS predictions.

**Figure 10:**(a) Bubble points of the ternary system methyl palmitate+hexadecanol+ hydrogen ( $x_{\text{HD}}:x_{\text{MP}}=1$ )  
(b) Bubble points of the ternary system hexadecanol+methanol+hydrogen ( $x_{\text{HD}}:x_{\text{Metanol}} = 1$ ) Dots: experimental data (11). — GCA-EoS predictions

**Figure 11:**(a) Phase diagram of the ternary system methyl palmitate+propane+hydrogen ( $x_{\text{H}_2}:x_{\text{MP}} = 4$ )  
(b) Bubble points of the ternary system hexadecanol+propane+hydrogen ( $x_{\text{H}_2}:x_{\text{HD}} = 4$ ) Dots: experimental data (10, 11). — GCA-EoS predictions.

**Table 1.** GCA-EOS model parameters

Term	Type	Parameter	
Repulsive	Molecular	Hard sphere diameter: $d_c$	Estimated
Attractive	Group	Reference temperature: $T^*$	Constant
		Surface area: $q_i$	Constant
		Energy $g_{ii}, g_{ii}', g_{ii}''$	Estimated
		Interaction: $k_{ij}, k_{ij}'$	Estimated
	Binaries	Non random: $\alpha_{ij}, \alpha_{ji}$	Estimated
Associative	Group	Association energy: $\varepsilon_i$	Constant
		Association volume $\kappa_i$	Constant

**Table 2:** Pure component properties

Compound	$d_c$ [cm mol <sup>-1</sup> ]	T <sub>c</sub> [K]
Hydrogen	2.672	33.2
Propane	4.017	369.8
n-Butane	4.362	425.18
Methanol	3.61	512.6
Methyl palmitate	7.695	735.9
n-Hexadecanol	7.376	770.
Tripalmitin*	11.44	1020.

\*dc obtained from Bottini et al (5) correlation



**Table 3:**GCA-EoS binary interactions parameters.

Group i	Group j	$k_{ij}^*$	$k_{ij}^?$	$\alpha_{ij}$	$\alpha_{ji}$	N	SDV%	Source
H <sub>2</sub>	CH <sub>2</sub> / CH <sub>3</sub>	1.0	0.0	11.846	11.846	63	1.263	(9)
H <sub>2</sub>	TG	1.0	0.0	-10.144	-10.144			

$$SDV\% = 100 \sqrt{\sum_N ((x_{calc} - x_{exp}) / x_{exp})^2 / N} \quad x = \text{liquid phase composition}$$

**Table 4:** GCA-EoS binary interaction parameters

Group j	Group i	$k_{ij}^*$	$k_{ij}'$	$\alpha_{ij}$	$\alpha_{ji}$	Source
CH <sub>2</sub> /CH <sub>3</sub>	CH <sub>2</sub> COO	0.8794	0.05024	4.045	-16.601	(10) <sup>1</sup> , (15) <sup>2</sup>
H <sub>2</sub>	CH <sub>2</sub> COO	1.0	0.0	0.879	0.879	(10) <sup>3</sup>
H <sub>2</sub>	CH <sub>2</sub> OH	0.9481	0.1138	-2.9583	-2.9583	(11) <sup>4</sup>
CH <sub>2</sub> COO	CH <sub>2</sub> OH	1.1649	0.0	-2.8298	-2.8298	(16), (17)

<sup>1</sup> Rovetto et al (10): C<sub>3</sub>H<sub>8</sub> + methyl palmitate (isopleth:  $x(\text{C}_3\text{H}_8) = 0.8011$ )

<sup>2</sup> Brands (15): C<sub>4</sub>H<sub>10</sub> + methyl palmitate (isopleth:  $x(\text{C}_4\text{H}_{10}) = 0.8627$ )

<sup>3</sup> Rovetto et al (10): H<sub>2</sub> + methyl palmitate (isopleths:  $x(\text{H}_2) = 0.0495$  and  $0.1284$ )

<sup>4</sup> Rovetto et al (11): H<sub>2</sub> + 1-hexadecanol (isopleths:  $x(\text{H}_2) = 0.0805$  and  $0.1025$ )

**Table 5:** Systems used for parameter estimation between the CH<sub>2</sub>COO and CH<sub>2</sub>OH groups

System	T(K)	N	$\Delta P\%$	$\Delta y\%$
1-propanol+methylpropanoate	328.15 -348.15	40	3.6537	6.0709
1-propanol+methylbutanoate	333.15 - 353.15	48	2.9346	2.5208
1-butanol+methylpropanoate	348.15	20	3.0878	6.8073
1-butanol+methylbutanoate	348.15 - 368.19	39	2.7996	3.4851

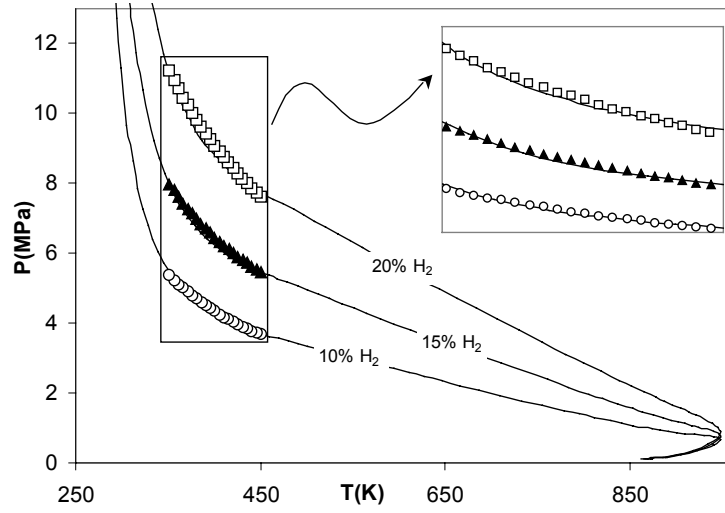


**Figure 1:** Phase diagram of the binary system hydrogen+tripalmitin.  
 Dots: experimental data (9); — GCA-EoS correlation

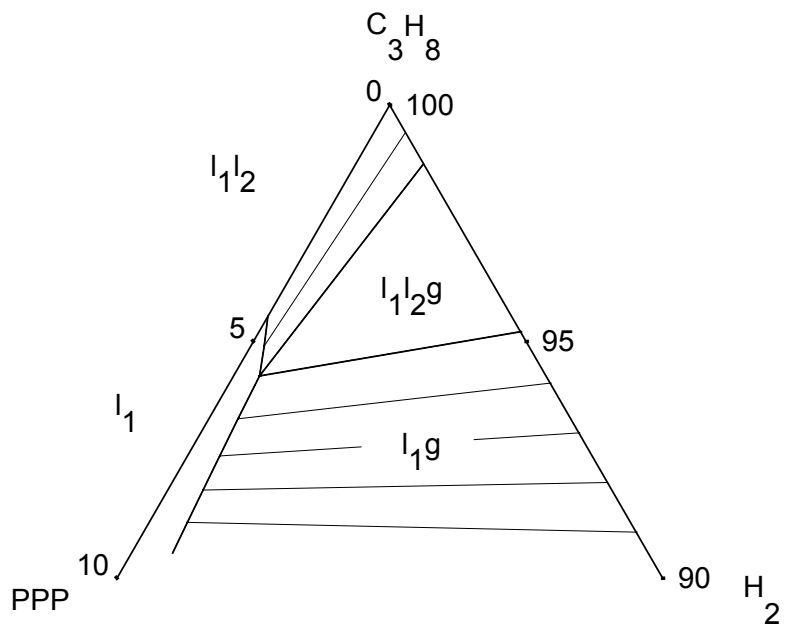


**Figure 2:** Immiscibility region for the ternary system hydrogen+tripalmitin (PPP)+propane at 360 K and 4 MPa.

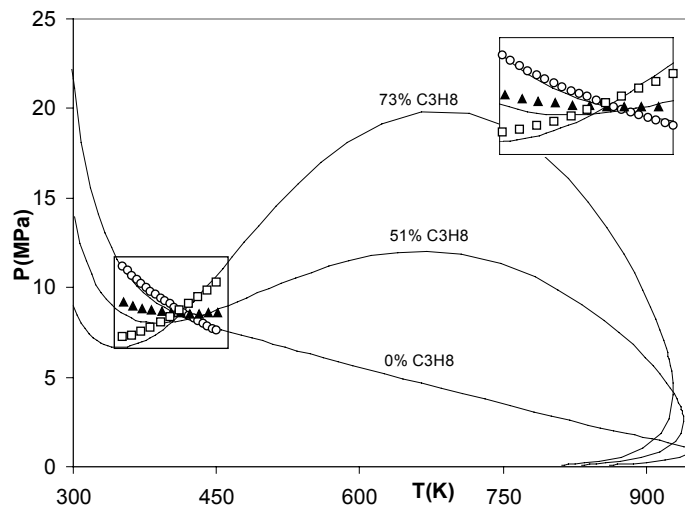


**Figure 3:** Phase diagram of the ternary system hydrogen+propane+tripalmitin(PPP) at a constant molar ratio  $x(\text{PPP})/x(\text{H}_2) = 4.15$  — GCA-EoS predictions. Dots: experimental data (9).

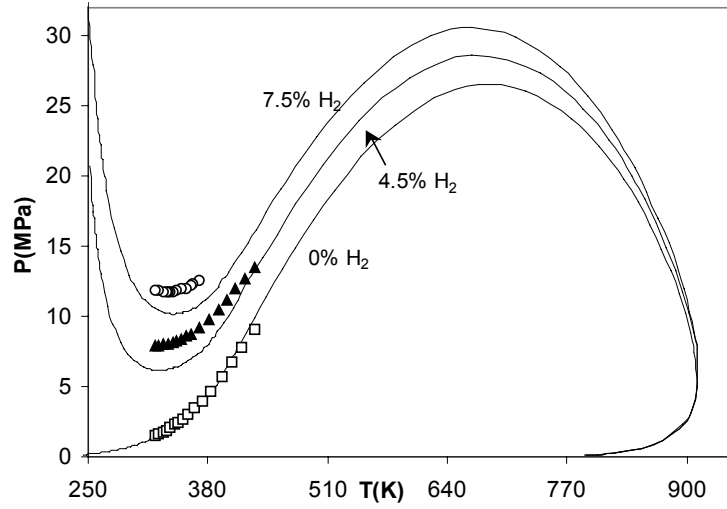


**Figure 4:** Phase diagram of the ternary system hydrogen+propane+tripalmitin at a constant molar ratio  $x(\text{C}_3\text{H}_8) / x(\text{PPP}) = 7$ . Dots: experimental data (9). — GCA-EoS predictions.

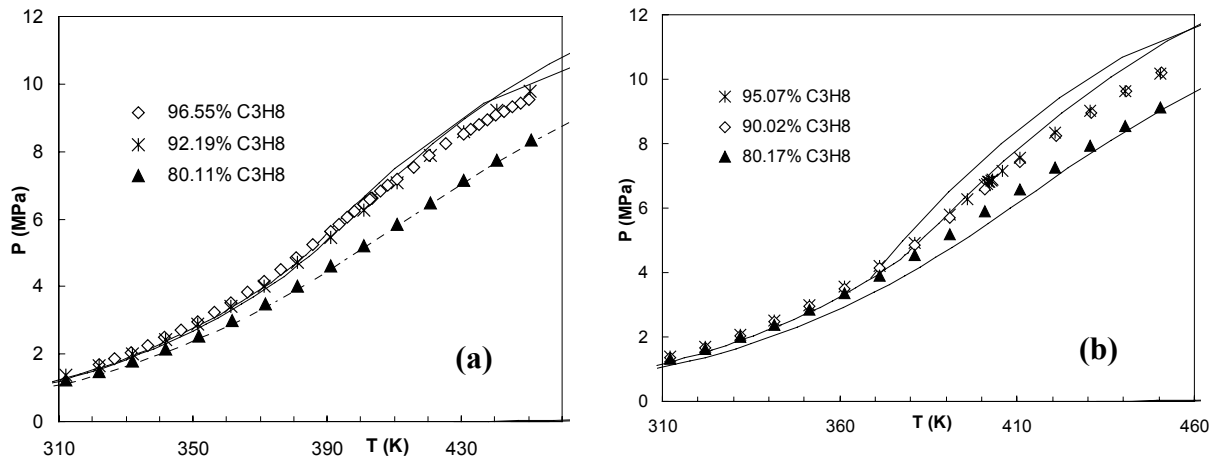


**Figure 5:** (a) Phase diagram of the binary system methyl palmitate+propane  
 (b) Phase diagram of the binary system hexadecanol+propane  
 Dots: experimental data (10, 11). - - - GCA-EoS correlation. — GCA-EoS predictions.



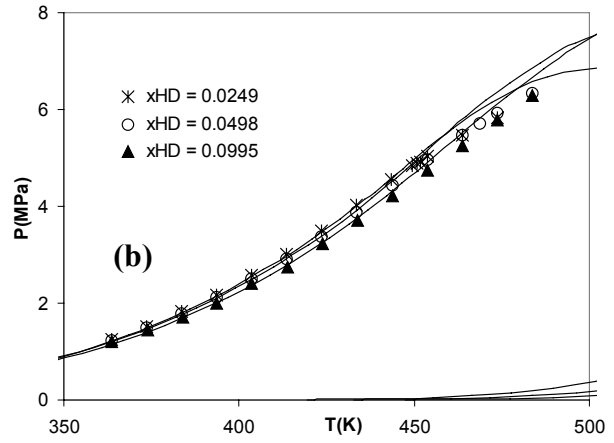
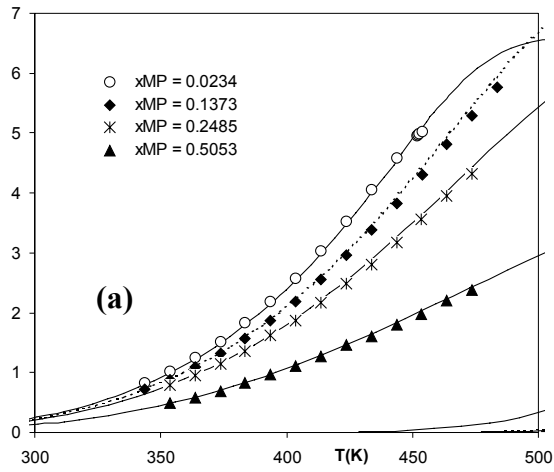


**Figure 6:** (a) Phase diagram of the binary system methyl palmitate(MP)+butane  
 (b) Phase diagram of the binary system hexadecanol(HD)+butane  
 Dots: experimental data (15). - - - GCA-EoS correlation. — GCA-EoS predictions.

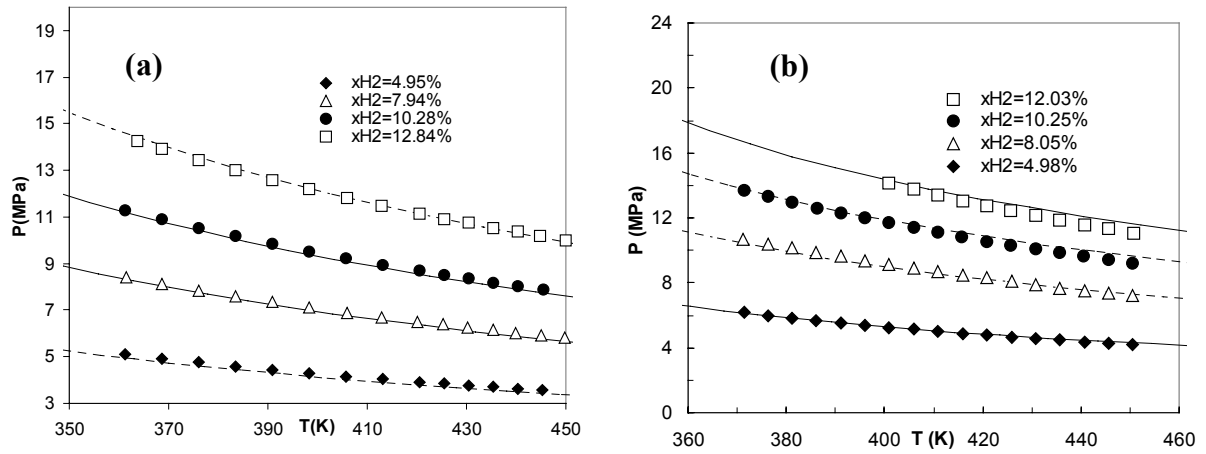


**Figure 7:** (a) Bubble points of the binary system methyl palmitate + hydrogen  
 (b) Bubble points of the binary system hexadecanol + hydrogen  
 Dots: experimental data (10, 11). - - - GCA-EoS correlations. — GCA-EoS predictions.

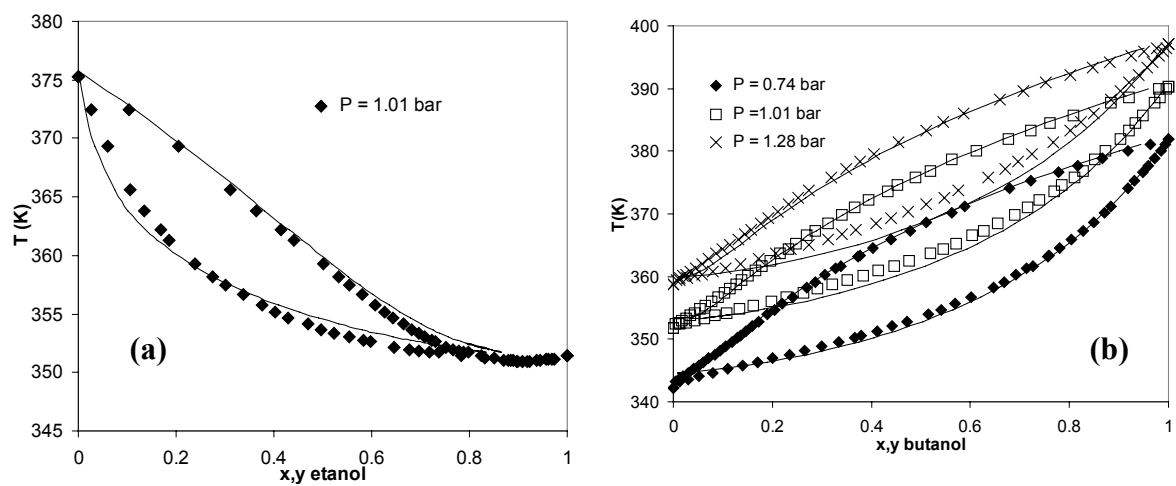


**Figure 8:** (a) Vapor-liquid equilibria of the binary system ethanol+methylbutanoate.  
 (b) Vapor-liquid equilibria of the binary system butanol+methylpropanoate.  
 Dots: experimental data (20, 21). — GCA-EoS predictions.

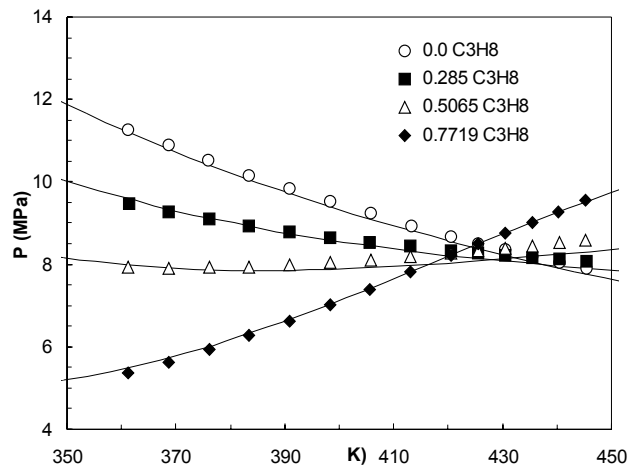


**Figure 9:** Bubble pressure of the ternary system methyl palmitate+hydrogen+propane ( $x_{MP} : x_{H_2} = 8.7$ )  
Dots: experimental data (10). — GCA-EoS predictions.

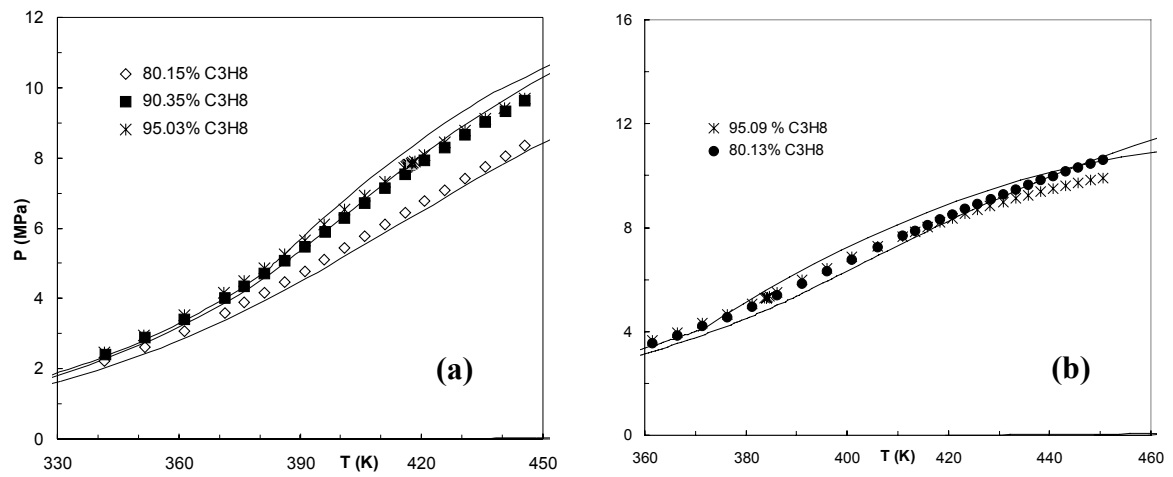


**Figure 10:**

**(a)** Bubble points of the ternary system methyl palmitate+hexadecanol+hydrogen ( $x_{HD}:x_{MP}=1$ )

**(b)** Bubble points of the ternary system hexadecanol+methanol+hydrogen ( $x_{HD}:x_{Metanol} = 1$ )

Dots: experimental data (11). — GCA-EoS predictions

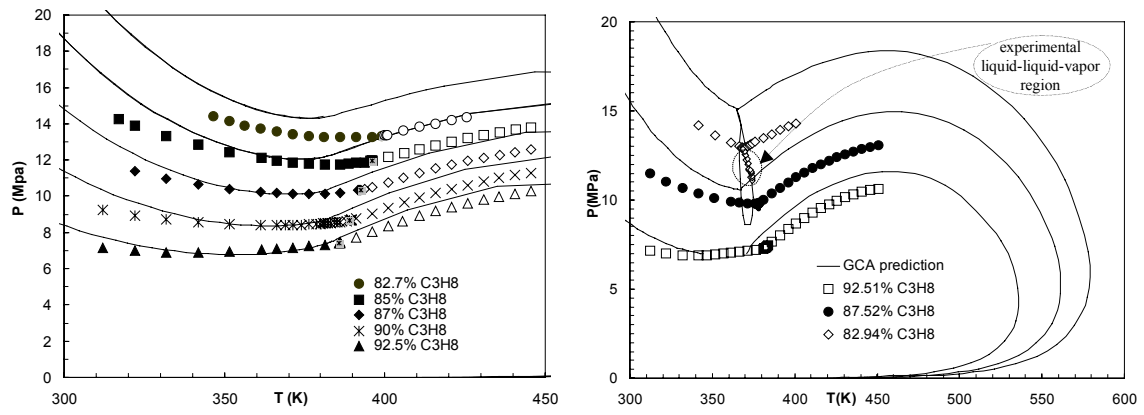


**Figure 11:**

(a) Phase diagram of the ternary system methyl palmitate+propane+hydrogen ( $x_{H_2} : x_{MP} = 4$ )

(b) Bubble points of the ternary system hexadecanol+propane+hydrogen ( $x_{H_2} : x_{HD} = 4$ )

Dots: experimental data (10, 11). — GCA-EoS predictions